

Study of carbide inserts in the milling of Hadfield steels

Alexey Pyatykh (✉ pyatykhas@ex.istu.edu)

Irkutsk National Technical Research University: Irkutskij nacional'nyj issledovatel'skij tehničeskij universitet <https://orcid.org/0000-0002-4116-9190>

Andrey Savilov

Irkutsk National Technical Research University: Irkutskij nacional'nyj issledovatel'skij tehničeskij universitet

Sergey Timofeev

Irkutsk National Technical Research University: Irkutskij nacional'nyj issledovatel'skij tehničeskij universitet

Research Article

Keywords: Hadfield steel, milling, cutting forces, coefficient of friction, Taguchi method, analysis of variance, regression analysis

Posted Date: April 19th, 2022

DOI: <https://doi.org/10.21203/rs.3.rs-1436702/v1>

License: © ⓘ This work is licensed under a Creative Commons Attribution 4.0 International License.

[Read Full License](#)

Abstract

Cutting of Hadfield steels has been a major problem and a real challenge for engineers due to its high toughness, ductility and capacity for work hardening. To solve this problem, it is important to choose an optimal cutting tool. Cutting force values should be compared in choosing the most effective tool. Different grades of carbide and protective coatings of indexable inserts have a different impact on the cutting dynamics and force due to different coefficients of friction between the insert surface and the chip. For a comparative analysis of inserts made of various hard materials, a variety of methods were applied. The Taguchi method was used to analyze the cutting process using the "less is more" quality and to determine the grade with the best properties. The variance analysis revealed the most important factor influencing the active cutting force - the tool feed. The regression analysis confirmed the results obtained at the previous stages and revealed avenues for further research.

Introduction

Hadfield steel belongs to austenitic manganese steels, which combine high toughness and ductility with high strain hardening capacity [1–4].

High-manganese austenitic steels containing 0.90–1.50% C and 11.50–15.00% Mn and highly wear resistant while being exposed to high pressures or shock loads have been widely used in various areas. Steel products are manufactured by casting into sand and metal molds, followed by heat treatment: steel is heated up to 1100°C and quenched in water [5]. After hardening, steel has a hardness of 250 HB. Under the influence of dynamic loads and cold deformation, steel is hardened up to HB 600. As a result, it becomes difficult to machine or non-machinable [6].

Hadfield steel is used in the manufacture of vortex and ball mills, crusher jaws, tram and railway switches and crosses, caterpillar tracks, sprockets, excavator bucket teeth and other impact wear resistant parts [7].

Properties of high-manganese steel such as high hardness, hardenability, surface hardening and low thermal conductivity create difficulties in the cutting process. Due to the high cutting forces and temperatures, tools become worn so rapidly that it is difficult to control the dimensional accuracy [8]. Therefore, research aimed at improving the efficiency of Hadfield steel machining is relevant.

End milling is the most common machining method for steel parts. Most studies on Hadfield steel machining deal with this process. However, this process remains understudied due to the high cost of cutting tools [9–11].

Tooling costs can be reduced by using cutters with inserts instead of solid ones. Mills with interchangeable inserts can be installed on inserts with different geometries and made of different materials. Since the hardness of Hadfield steel in the initial state is 250 HB, the best material for wear inserts is hard alloy [12].

Along with tool life and surface roughness, one more important milling parameter is the cutting force [13]. To improve the machining productivity and reduce loads on technological systems, it is necessary to determine the geometry of cutting tools and machining parameters at which the cutting force is minimal. A limited number of studies have dealt with end milling of Hadfield steel [14–16]. These studies have not analyzed the impact of insert materials on the cutting force.

When choosing hard material brands, cutting tooling manufacturers take into account both the chemical composition and structures of materials and types of protective coating. Different protective coatings have different coefficients of friction when chips are moving along the back and front surfaces of the insert. Accordingly, different coefficients of friction affect the cutting force.

Changes in the cutting parameters modify the conditions for chip contact with the front and back insert surfaces. This is due to a change in temperatures, shapes and types of chips [17, 18]. These factors depend on the cutting speed, feed, depth and width of cut.

The issues of chip and tool surface contact are considered in the studies of chip shrinkage and cutting force control [19–21]. These studies analyze the impact of cutting parameters and tool geometries on the chip shrinkage coefficient. However, they ignore the role of tool protective coatings for the chip moving over the tool surface.

The research method selected for the present study plays an important role in obtaining objective results. Along with the mathematical modeling, experimental methods are used. The most common methods include the Taguchi method and the variance and regression analyses. They have both advantages and disadvantages [12, 22–24]. The use of several methods can improve the reliability of results.

The purpose of this work is to study the effect of various types of protective coating on the cutting force. To achieve this goal, the Taguchi method and the variance and regression analyses were used.

Methods And Results

The experiments were conducted on the CNC milling center DMG DMU80P. The block with dimensions of 145 × 100 × 80 mm made of Hadfield steel (110G13L) was used as a workpiece. The chemical composition is presented in Table 1. The workpiece was fastened on the Kistler 9253B multicomponent dynamometer insert installed on the machine table (Fig. 1). Using this insert, the cutting forces were measured. The milling direction was associated; the cutting pattern was ledge-type. Experimental cuts were made at three different cutting speeds $V_c=90, 120$ and 150 m/min and three different feeds $f_z=0.09, 0.12$ and 0.15 mm/rev.

The Sandvik R390-020C3-11M050 cutter was used as a cutting tool. Inserts R390-11 T3 31M-PM of the same geometry, made of S30T, S40T, 1130 and 4240 hard alloys were alternately installed on the cutter (Table 2). Each carbide grade has a unique protective coating and chemical composition. Each type of

coating was applied by different methods. In order to eliminate the influence of the cutting edge, only one insert was installed [12].

Table 2
Insert parameters

Parameters	Grade			
	S30T	S40T	1130	4240
Coating	PVD TiAlN	CVD TiCrN + Al ₂ O ₃ + TiN	PVD AlTiCrN	CVD TiCN + Al ₂ O ₃ + TiN
Corner radius (mm)	3.1	3.1	3.1	3.1
Effective length of the cutting edge (mm)	10	10	10	10
Major cutting edge angle (deg)	90	90	90	90

Cutting forces F_x , F_y and F_z were measured in the milling process. The milling scheme and cutting force directions are shown in Fig. 2.

With the cutting insert wear, the axial and active forces increase. The active cutting force F_a was calculated taking into account that $F_x=F_f$, $F_y=F_{fN}$ using formula $F_a = \sqrt{F_f^2 + F_{fN}^2}$.

The experiment was planned based on the robust plan Taguchi L 18 ($2^1 \times 3^2$). The Taguchi method involves the use of the signal-to-noise ratio to characterize the process. The signal is a change in the properties of product y under the influence of controlled factors x , and noise is a deviation of y (characterized by variance s^2) due to the influence of uncontrolled factors z . There are several qualities to analyze the process [25]:

1. The logarithmic function of variance:

$$\frac{S}{N} = -10 \log s^2$$

2. The signal-to-noise ratio:

$$\frac{S}{N} = 10 \left(\frac{y^2}{s^2} \right)$$

3. More-less:

$$\frac{S}{N} = -10 \log \left[\frac{\sum y^{-2}}{n} \right]$$

4. Smaller-better:

$$\frac{S}{N} = -10 \log \left[\frac{\sum y^2}{n} \right]$$

In the current study, the “Less is better” quality was used.

A change in the active force F_a under the influence of controlled factors acted as a signal: A was the alloy grade, B was the cutting speed, C was the feed, and F_a deviation was the noise.

Carbide inserts of S30T, S40T and 1130, 4240 grades, cutting speed V_c , feed f_n ($f_n=f_z$) were selected as variable parameters, whose values are presented in Tables 3 and 4. The milling parameters were determined based on the cutting tool manufacturer's recommendations.

Table 3
Milling parameters and their levels.

Parameters	Symbol	Level 1	Level 2	Level 3
Grade	A	S30T	1130	–
Cutting speed, V_c (m/min)	B	90	120	150
Feed rate, f_n (mm/rev)	C	0.09	0.12	0.15

Table 4
Milling parameters and their levels.

Parameters	Symbol	Level 1	Level 2	Level 3
Grade	A	S40T	4240	–
Cutting speed, V_c (m/min)	B	90	120	150
Feed rate, f_n (mm/rev)	C	0.09	0.12	0.15

For each pair of hard material inserts, the experiment was based on a mixed orthogonal matrix (Table 5). The experimental plan and values of the cutting parameters are presented in Tables 6–7.

Table 5
The factorial plan with an orthogonal array Taguchi
 $L_{18}(2^1 \times 3^2)$

Experiment no.	Factor A	Factor B	Factor C
1	1	1	1
2	1	1	2
3	1	1	3
4	1	2	1
5	1	2	2
6	1	2	3
7	1	3	1
8	1	3	2
9	1	3	3
10	2	1	1
11	2	1	2
12	2	1	3
13	2	2	1
14	2	2	2
15	2	2	3
16	2	3	1
17	2	3	2
18	2	3	3

Table 6
The experiment results (S30T and 1130)

Experiment no.	Control factors			Active force, Fa (N)	Fa for S/N ratios
	A	B	C		
	Grade	Cutting speed (Vc)	Feed rate (fn)		
1	S30T	90	0.09	262,8	-48,3933
2	S30T	90	0.12	338,7	-50,5971
3	S30T	90	0.15	384,9	-51,7059
4	S30T	120	0.09	257,7	-48,2223
5	S30T	120	0.12	319,9	-50,0997
6	S30T	120	0.15	373,3	-51,4414
7	S30T	150	0.09	255,1	-48,1349
8	S30T	150	0.12	287,6	-49,1768
9	S30T	150	0.15	355,8	-51,0233
10	1130	90	0.09	317,0	-50,0208
11	1130	90	0.12	345,1	-50,7591
12	1130	90	0.15	407,3	-52,1976
13	1130	120	0.09	299,5	-49,5291
14	1130	120	0.12	358,1	-51,0791
15	1130	120	0.15	342,4	-50,6899
16	1130	150	0.09	255,6	-48,1495
17	1130	150	0.12	300,2	-49,5470
18	1130	150	0.15	347,3	-50,8151

Table 7
The experiment results (S40T and 4240)

Experiment no.	Control factors			Active force, Fa (N)	Fa for S/N ratios
	A	B	C		
	Grade	Cutting speed (Vc)	Feed rate (fn)		
1	S40T	90	0.09	337,5	-50,5650
2	S40T	90	0.12	395,0	-50,5650
3	S40T	90	0.15	451,1	-50,5650
4	S40T	120	0.09	324,2	-50,5650
5	S40T	120	0.12	401,8	-50,5650
6	S40T	120	0.15	409,5	-50,5650
7	S40T	150	0.09	274,2	-50,5650
8	S40T	150	0.12	316,4	-50,5650
9	S40T	150	0.15	360,7	-50,5650
10	4240	90	0.09	393,1	-50,5650
11	4240	90	0.12	650,8	-50,5650
12	4240	90	0.15	398,2	-50,5650
13	4240	120	0.09	318,8	-50,5650
14	4240	120	0.12	361,9	-50,5650
15	4240	120	0.15	392,6	-50,5650
16	4240	150	0.09	463,6	-50,5650
17	4240	150	0.12	315,6	-50,5650
18	4240	150	0.15	340,1	-50,5650

The influence of variable parameters on the active cutting force was analyzed using the "S/N response table" (Table 8 and Table 9). The tables show optimal values of the variable parameters for the minimum active cutting force. The values of the control factors for Fa shown in Tables 8 and 9 are presented in Figs. 3 and 4. The graphs were used to determine optimal values of the control factors to minimize the active cutting force. The best level for each control factor was determined for the highest S/N ratio. The S/N levels and ratios for the factors providing the lowest Fa value are: for the group of S30T and 1130 carbide inserts, for factor A -level 1, S/N=-49.87, for factor B -level 3, S/ N=-49.47), for factor C – level 1,

S/N=-48.74; for the group of S40T and 4240 inserts, for factor A -level 1, S/N=-51.12, for factor B -level 3, S/N=-50.64-), for factor C – level 1, S/N =-50.80.

Table 8
S/N response table for Fa factor
(S30T and 1130)

Level	A	B	C
1	-49.87	-50.61	-48.74
2	-50.31	-50.18	-50.21
3	-	-49.47	-51.31
Delta	0.44	1.14	2.57

Table 9
S/N response table for Fa factor
(Grade S40T and 4240)

Level	A	B	C
1	-51.12	-52.62	-50.80
2	-51,91	-51,28	-51.91
3	-	-50.64	-51.83
Delta	0.80	1.98	1.10

Based on the data in Tables 8 and 9 and the graphs in Figs. 3 and 4, the optimum Fa value was determined for milling with a S30T carbide insert ($V_c = 150$ m/min and $f_z = 0.09$ mm/ tooth) and a S40T carbide insert ($V_c = 150$ m/min and $f_z = 0.09$ mm/tooth).

Using the results obtained, S30T and S40T carbide inserts were compared. The results are presented in Table 10 and Fig. 5. An analysis of the levels and S/N ratios revealed that in milling of Hadfield steel, S30T carbide inserts with a minimum S/N ratio of 49.87 should be used.

Table 10
S/N response table for Fa factor
(S30T and 1130)

Level	A	B	C
1	-49.87	-51.05	-49.05
2	-51.12	-50.72	-50.65
3	-	-49.71	-51.77
Delta	1.25	1.34	2.72

The variance analysis is used to determine the individual interactions of all controlled factors. In the current study, the variance analysis was used to study the effect of carbide inserts, cutting speed and feed on the active cutting force. The results are presented in Table 11. The analysis was carried out with a significance level of 5% and a confidence level of 95%. Table 11 shows that the percentage contributions of factors A, B, and C to the active cutting force were 21.37%, 7.45%, and 65.22%, respectively. Thus, the most important factor influencing the active cutting force was the tool feed (factor C, 65.22%). The error rate was significantly lower – 5.95%.

Table 11
Results of ANOVA for the Active Cutting Force

Variance source	Degree of freedom (DoF)	Sum of squares (SS)	Mean square (MS)	F-Value	Contribution rate (%)
<i>F_a</i>					
A	1	10500	10500	3.69	21.37
B	2	9196	3123	1.47	7.45
C	2	32557	16278	10.40	65.22
Error	51	10805	211.9		5.95
Total	53	181297			100

The regression analysis was applied to model and analyze dependent and independent variables. The dependent variable is active cutting force F_a ; the independent variables are cutting speed and tool feed. The prognostic equation is presented below. The values of the coefficient of equation determination, which was obtained using the linear regression model for F_a , were 91.82% and 90.07%, respectively.

$$F_a = 165,6 + 48,30 A - 0,890 B + 1732 C$$

$$R\text{-Sq} = 91.82\% \quad R\text{-Sq}(\text{adj}) = 90.07\%$$

Figure 6 compares the actual test results and the predicted values obtained using the linear regression model. As can be seen, there is a relationship between the predicted values and the test results.

The dependences of cutting forces on cutting data obtained by the regression analysis are shown in Fig. 7. The graph for the S30T grade (Fig. 7a) shows that the dependence of cutting force on feed and cutting speed is linear for all the cutting data. With an increase in the feed, the cutting force increases proportionally, which is consistent with the cutting theory. With an increase in the cutting speed, the cutting force decreases due to a decrease in the strength of the material affected by the temperature in the cutting zone, which grows with increasing cutting speed values. These results make it possible to predict values of the cutting force when using S30T grade inserts. If the satisfactory tool life is achieved at maximum cutting parameters, S30T inserts can be used for machining Hadfield steel parts.

The graph for the S40T grade (Fig. 7b) shows that the dependence of cutting forces on feed is close to linear and cutting force values are higher than for the S30T grade over the entire feed range. The dependence of cutting forces on cutting speed is parabolic, reaching maximum values in the speed range $V_c=110-115$ m/min. It can be assumed that in the specified range of cutting speeds, the build-up of material affects the cutting edge. When using S40T inserts at maximum feed values, the cutting force is higher by about 5%.

The dependences of cutting forces on feed and cutting speed for 1130 grade inserts (Fig. 7c) are similar to the dependences obtained for S30T grade inserts. At the same time, the cutting forces measured at maximum cutting parameters are approximately 4% lower than those for S30T grade inserts. These results indicate that the 1130 grade is a promising tool material for Hadfield steel. Along with the S30T alloy, it requires additional testing for durability.

The cutting force plot for the 4240 grade (Fig. 7d) is non-linear. The hyperbolic dependence of cutting forces on cutting speed is combined with a parabolic dependence on feed. This indicates a significant influence of cutting modes on the chip interacting with the insert surface. This fact makes it difficult to predict changes in cutting forces depending on the cutting parameters. When using the 4240 grade, the cutting force exceeds the one measured when using other alloys. The minimum value of the cutting force was measured at $V_c=120$ m/min. This means that in some cases the machining performance should be reduced by at least 30% in order to ensure a minimum load on the technological system.

Conclusion

In this study, various experimental methods were applied to select the most effective carbide inserts in milling of Hadfield steel.

When using the Taguchi method, the analysis used the "Less is more" quality. The S/N ratios for the active cutting force were found during the experiments conducted on the orthogonal matrix. It was concluded that in terms of the active cutting force the best choice in milling of Hadfield steel is S30T inserts.

The variance analysis showed that the most important factor affecting the active cutting force is tool feed. The share of feed was 65.22%. The error was 5.95%, which can be considered acceptable.

The regression analysis found that in order to reduce values of the cutting force and predict cutting forces over the entire range of the cutting parameters, the S30T alloy is more preferable. The 1130 grade is also promising. Both alloys are recommended for durability tests, which will determine the possibility of applying them in real production conditions.

The build-up and temperature effects on the cutting force can be avenues for further research.

Declarations

Acknowledgements

Not applicable.

Authors' contributions

AP was in charge of the whole trial; AS and AP wrote the manuscript; ST assisted with design of the experiment and conducting the analysis. All authors read and approved the final manuscript.

Authors' Information

Alexey Pyatykh, born in 1990, received his PhD degree on technical sciences in *Irkutsk National Research Technical University, Russia*, in 2019.

Currently Associate Professor at the *Department of Technology and Equipment for Machine-Building Productionh, Irkutsk National Research Technical University, Russia*.

Andrey Savilov, born in 1966, is currently Associate Professor at the *Department of Technology and Equipment for Machine-Building Productionh, Scientific Director of the High Performance Machining Lab, Irkutsk National Research Technical University, Russia*.

Sergey Timofeev, born in 1990, is currently a junior researcher at the *Department of Technology and Equipment for Machine-Building Production, Irkutsk National Research Technical University, Russia*.

Funding

Not applicable.

Competing interests

The authors declare no competing financial interests.

Author Details

¹Department of Technology and Equipment for Machine-Building Production, High Performance Machining Lab, Irkutsk National Research Technical University, Irkutsk 664074, Russia.

References

1. Tasker, J., & Amuda, M. O. H. (2017). Austenitic Steels: Non-Stainless. Reference Module in Materials Science and Materials Engineering. <https://doi.org/10.1016/B978-0-12-803581-8.09206-7>
2. Luo, K., & Bai, B. (2010). Microstructure, mechanical properties and high stress abrasive wear behavior of air-cooled MnCrB cast steels. *Materials & Design (1980–2015)*, *31*(5), 2510–2516. <https://doi.org/10.1016/J.MATDES.2009.11.040>

3. Chen, C., Lv, B., Ma, H., Sun, D., & Zhang, F. (2018). Wear behavior and the corresponding work hardening characteristics of Hadfield steel. *Tribology International*, 121(September 2017), 389–399. <https://doi.org/10.1016/j.triboint.2018.01.044>
4. Olawale, J. O., & Ibitoye, S. A. (2018). Failure analysis of a crusher jaw. *Handbook of Materials Failure Analysis*, 187–207. <https://doi.org/10.1016/B978-0-08-101928-3.00010-0>
5. Sinitskiy, Y.V., Nefedev, A.A, Akhmetova, A.A., Ovchinnikova, M.V., Hrenov, I.B., & Deryabin, D.A. (2016). Review of results of investigations aimed at improvement of properties of castings made from high manganese steel. *The theory and process engineering of metallurgical production*. 2(19), 45–57.
6. Hodzhibergenov, D. T., Sherov, K. T., Kasenov, A. Zh., Hozhibergenova, U. D. (2018). Problems of the choice of technology for processing of new intensified materials in manufacture. *Science and Technology of Kazakhstan*. 2. 111–117.
7. Varela, L. B., Tressia, G., Masoumi, M., Bortoleto, E. M., Regattieri, C., & Sinatora, A. (2021). Roller crushers in iron mining, how does the degradation of Hadfield steel components occur? *Engineering Failure Analysis*, 122, 105295. <https://doi.org/10.1016/J.ENGFAILANAL.2021.105295>
8. Horng, J. T., Liu, N. M., & Chiang, K. T. (2008). Investigating the machinability evaluation of Hadfield steel in the hard turning with Al₂O₃/TiC mixed ceramic tool based on the response surface methodology. *Journal of Materials Processing Technology*, 208(1–3), 532–541. <https://doi.org/10.1016/J.JMATPROTEC.2008.01.018>
9. Sousa, V. F. C., Silva, F. J. G., Alexandre, R., Fecheira, J. S., & Silva, F. P. N. (2021). Study of the wear behaviour of TiAlSiN and TiAlN PVD coated tools on milling operations of pre-hardened tool steel. *Wear*, 476, 203695. <https://doi.org/10.1016/J.WEAR.2021.203695>
10. Airao, J., Chaudhary, B., Bajpai, V., & Khanna, N. (2018). An Experimental Study of Surface Roughness Variation in End Milling of Super Duplex 2507 Stainless Steel. *Materials Today: Proceedings*, 5(2), 3682–3689. <https://doi.org/10.1016/J.MATPR.2017.11.619>
11. Kar, B. C., Panda, A., Kumar, R., Sahoo, A. K., & Mishra, R. R. (2020). Research trends in high speed milling of metal alloys: A short review. *Materials Today: Proceedings*, 26, 2657–2662. <https://doi.org/10.1016/J.MATPR.2020.02.559>
12. Kivak, T. (2014). Optimization of surface roughness and flank wear using the Taguchi method in milling of Hadfield steel with PVD and CVD coated inserts. *Measurement: Journal of the International Measurement Confederation*, 50(1), 19–28. <https://doi.org/10.1016/j.measurement.2013.12.017>
13. Shah, D. R., Pancholi, N., Gajera, H., & Patel, B. (2022). Investigation of cutting temperature, cutting force and surface roughness using multi-objective optimization for turning of Ti-6Al-4 V (ELI). *Materials Today: Proceedings*, 50, 1379–1388. <https://doi.org/10.1016/J.MATPR.2021.08.285>
14. Wojciechowski, S., Twardowski, P., & Wieczorowski, M. (2014). Surface texture analysis after ball end milling with various surface inclination of hardened steel. *Metrology and Measurement Systems*, 21(1), 145–156. <https://doi.org/10.2478/MMS-2014-0014>
15. Wojciechowski, S., W. Maruda, R., M. Krolczyk, G., & Niestony, P. (2018). Application of signal to noise ratio and grey relational analysis to minimize forces and vibrations during precise ball end milling.

- Precision Engineering, 51, 582–596. <https://doi.org/10.1016/J.PRECISIONENG.2017.10.014>
16. Philip, S. D., Chandramohan, P., & Rajesh, P. K. (2015). Prediction of surface roughness in end milling operation of duplex stainless steel using response surface methodology. *Journal of Engineering Science and Technology*, 10(3), 340–352.
 17. San-Juan, M., Martín, de Tiedra, M. D. P., Santos, F. J., López, R., & Cebrián, J. A. (2015). Study of Cutting Forces and Temperatures in Milling of AISI 316L. *Procedia Engineering*, 132, 500–506. <https://doi.org/10.1016/J.PROENG.2015.12.525>
 18. Tressia, G., Penagos, J. J., & Sinatora, A. (2017). Effect of abrasive particle size on slurry abrasion resistance of austenitic and martensitic steels. *Wear*, 376–377, 63–69. <https://doi.org/10.1016/J.WEAR.2017.01.073>
 19. Lomaeva, T. v., & Kugultinov, S. D. (2021). Investigation of cutting modes effect on cutting force while machining titanium alloy BT6 (Russian State Standard GOST 19807-91). *Materials Today: Proceedings*, 38, 1307–1309. <https://doi.org/10.1016/J.MATPR.2020.08.088>
 20. Altintas, Y. (2012). Manufacturing Automation. In *Journal of the Japan Society of Precision Engineering* (Vol. 380). <https://doi.org/10.2493/jjspe1933.48.945>
 21. Tounsi, N., & Otho, A. (2000). Dynamic cutting force measuring. *International Journal of Machine Tools and Manufacture*, 40(8), 1157–1170. [https://doi.org/10.1016/S0890-6955\(99\)00117-0](https://doi.org/10.1016/S0890-6955(99)00117-0)
 22. Zhang, J. Z., Chen, J. C., & Kirby, E. D. (2007). Surface roughness optimization in an end-milling operation using the Taguchi design method. *Journal of Materials Processing Technology*, 184(1–3), 233–239. <https://doi.org/10.1016/J.JMATPROTEC.2006.11.029>
 23. Asiltürk, I., & Akkuş, H. (2011). Determining the effect of cutting parameters on surface roughness in hard turning using the Taguchi method. *Measurement*, 44(9), 1697–1704. <https://doi.org/10.1016/J.MEASUREMENT.2011.07.003>
 24. Balaji, M., Murthy, B. S. N., & Rao, N. M. (2016). Optimization of Cutting Parameters in Drilling of AISI 304 Stainless Steel Using Taguchi and ANOVA. *Procedia Technology*, 25, 1106–1113. <https://doi.org/10.1016/J.PROTCY.2016.08.217>
 25. Gardiner, W. P., & Gettinby, G. (1998). Taguchi Methods. *Experimental Design Techniques in Statistical Practice*, 289–321. <https://doi.org/10.1533/9780857099785.289>

Tables

Tables 1 is not available with this version.

Figures

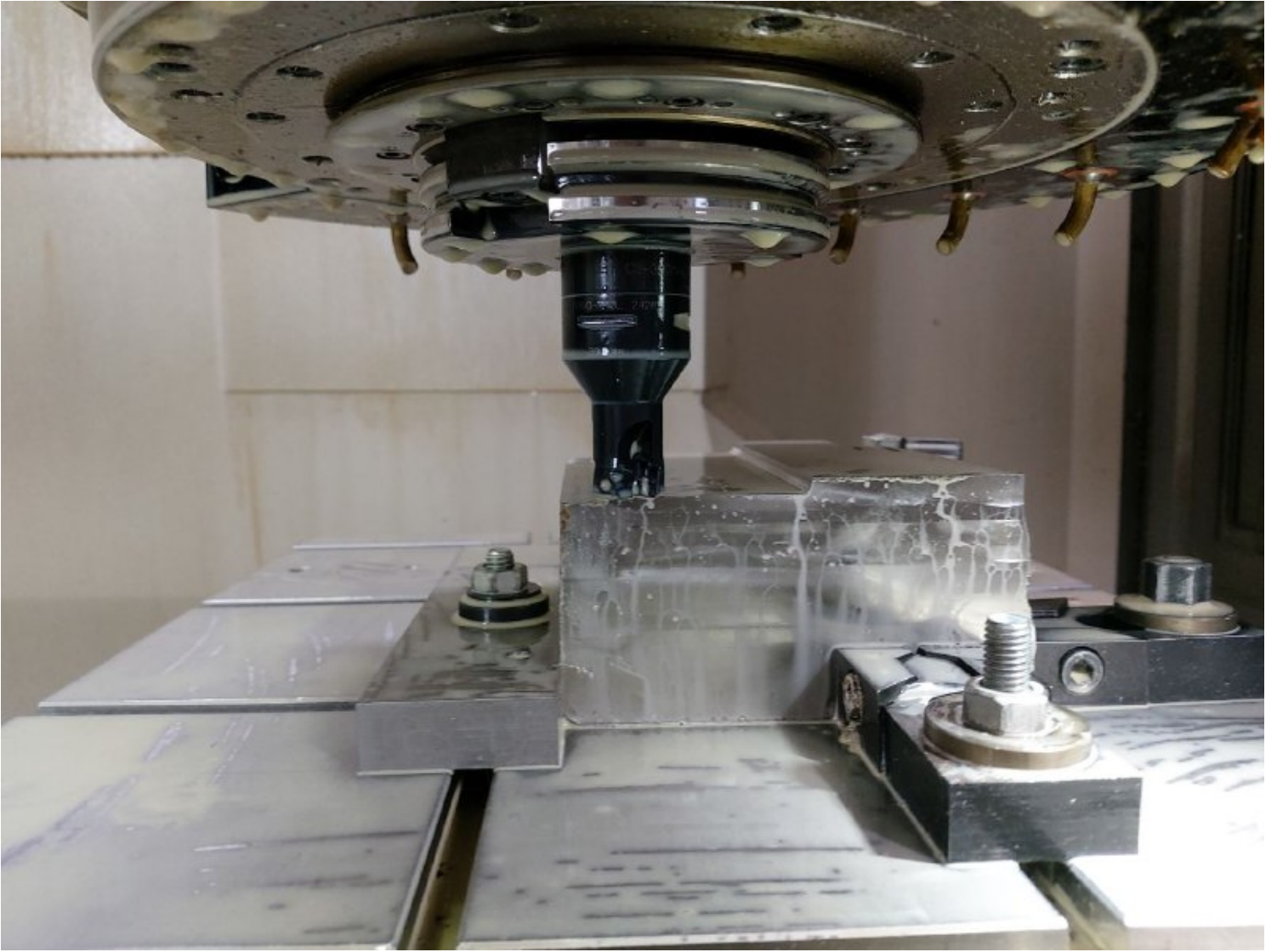


Figure 1

Working area of the DMU80P

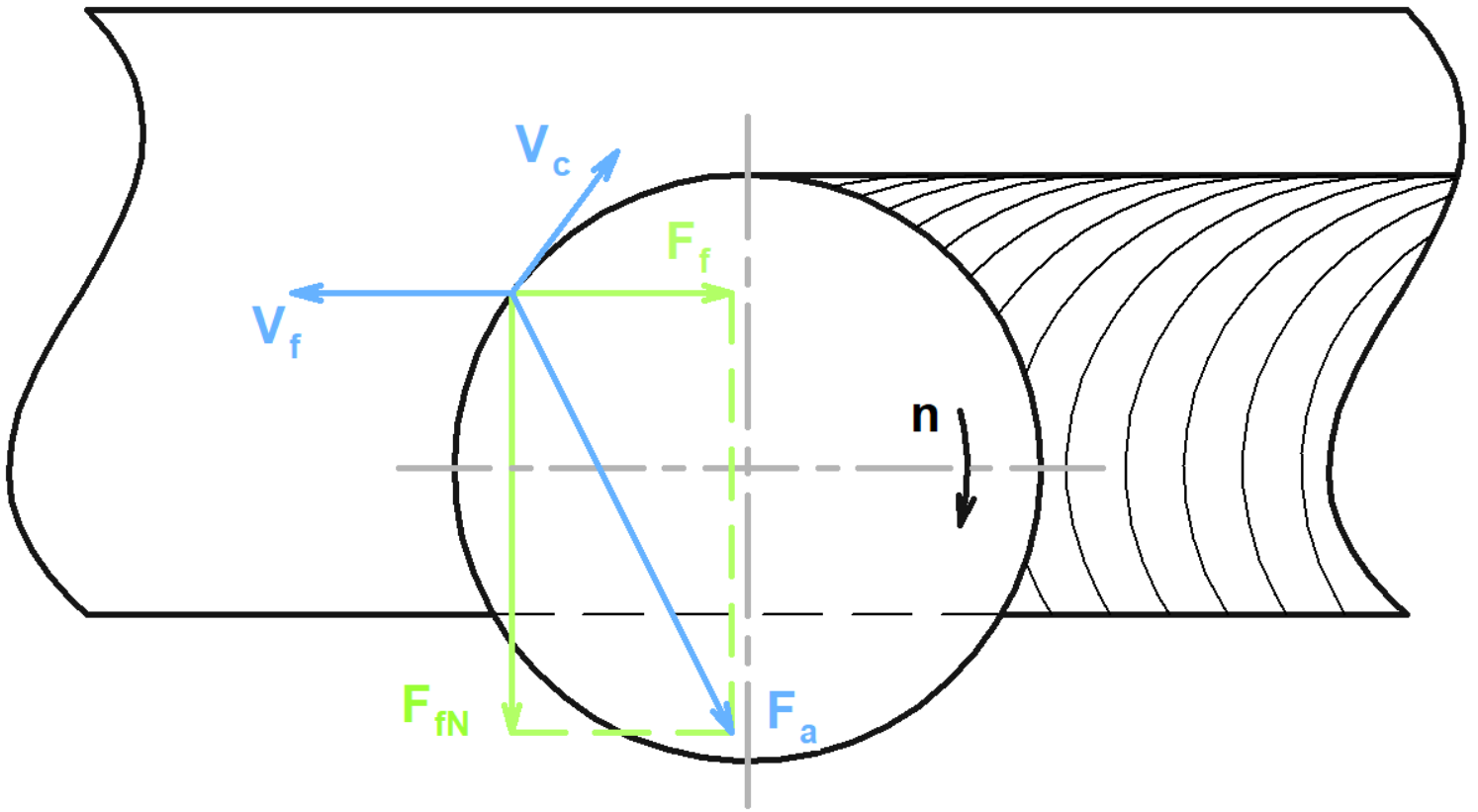


Figure 2

Cutting forces

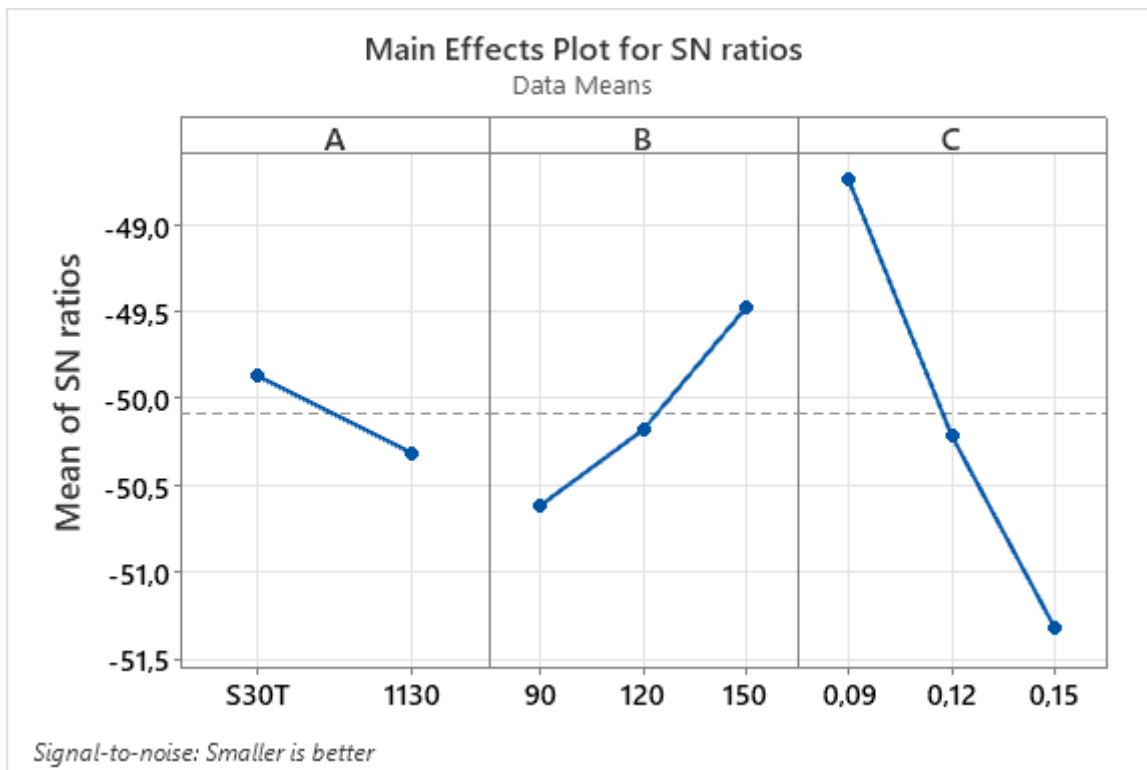


Figure 3

The graphic of mean S/N ratios versus factor levels (Fa). S30T and 1130 grades

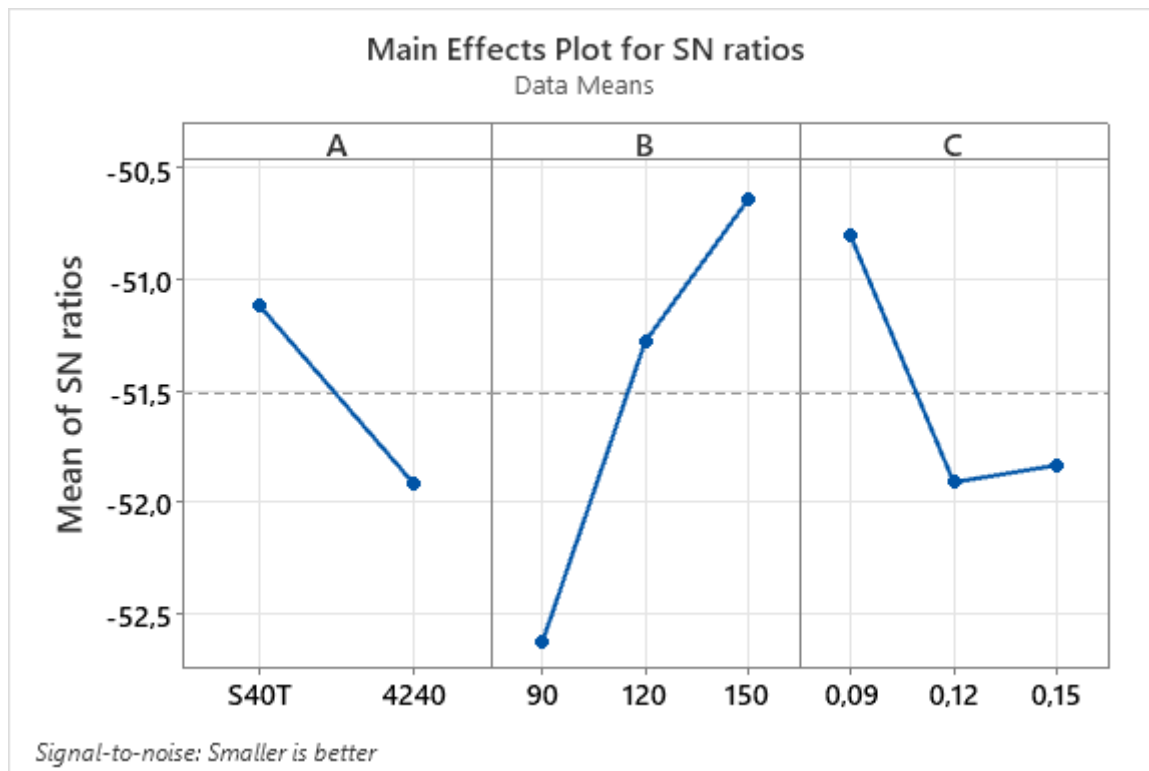


Figure 4

The graphic of mean S/N ratios versus factor levels (Fa). S40T and 4240 grades

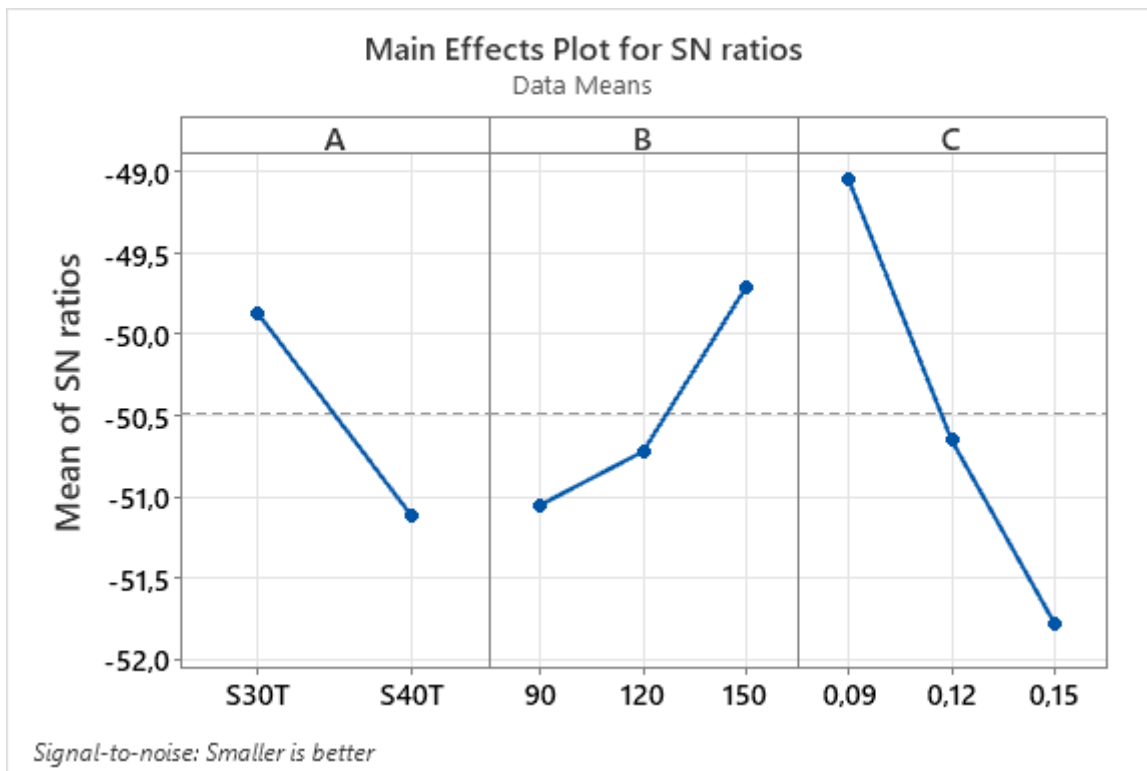


Figure 5

The graphic of mean of S/N ratios versus factor levels (Fa). Grade S30T and S40T

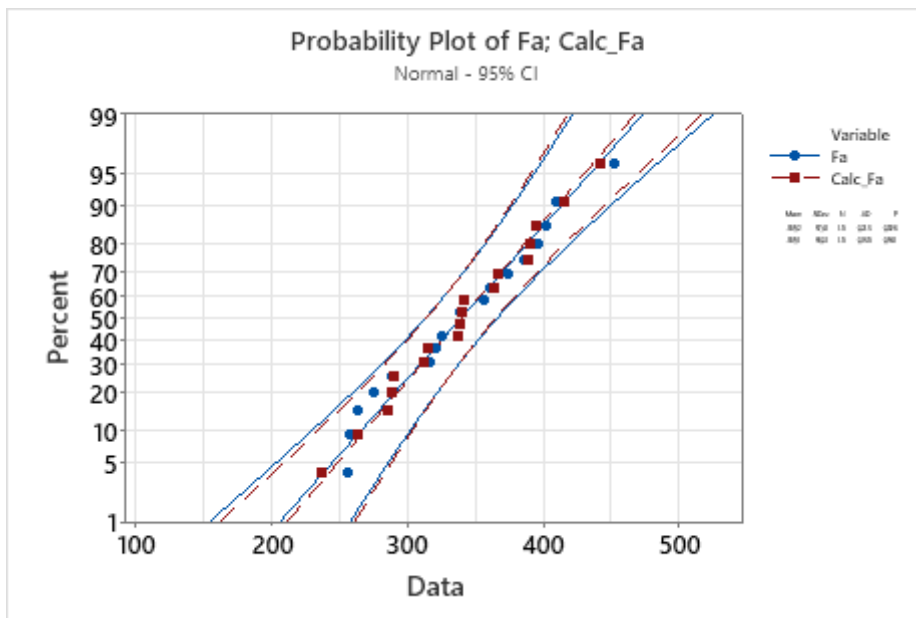


Figure 6

The comparison of the linear regression model with the experimental results

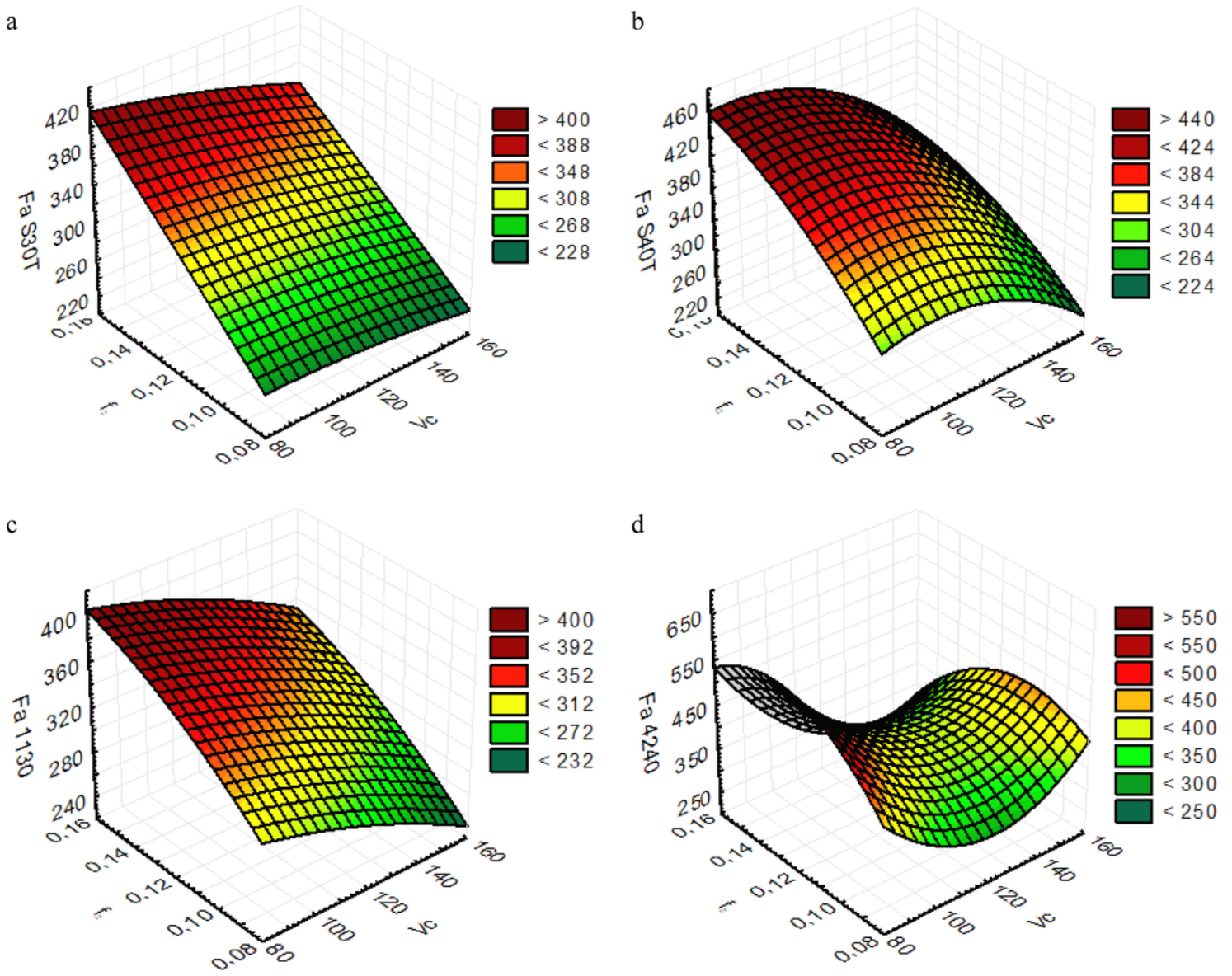


Figure 7

The impact of the cutting parameters on the active cutting force in milling with a - S30T inserts, b - S40T inserts, c – 1130 inserts, d – 4240 inserts